Low-recycling conditions and improved core confinement in steady-state operation scenarios in JET (Joint European Torus)

2013 Plasma Phys. Control. Fusion 55 045005

(http://iopscience.iop.org/0741-3335/55/4/045005)

IOP Publishing — Plasma Physics and Controlled Fusion

Plasma Phys. Control. Fusion **55** (2013) 045005 (14pp) doi:10.1088/0741-3335/55/4/045005

Low-recycling conditions and improved core confinement in steady-state operation scenarios in JET (Joint European Torus)

R Cesario[1], L Amicucci[2], A Fonseca[3], I T Chapman[4], F Jenko[5], M Marinucci[1], S Saarelma[4], P Smeulders[1], D Told[5], R Zagorski[6], Y Baranov[4], M Beurskens[4], R De Angelis[1], D Mc Donald[4], C Challis[3], A Galli[2], J Mailloux[3], V Pericoli[1], M Zerbini[1] and the EFDA-JET Contributors[7,8]

[1] Associazione EURATOM/ENEA sulla Fusione, Centro Ricerche Frascati c.p. 65, 00044 Frascati, Italy
[2] Università di Roma La Sapienza, Facoltà di Ingegneria, Via Eudossiana, Roma, Italy
[3] Associação EURATOM/IST Centro de Fusão Nuclear, 1049-001 Lisbon, Portugal
[4] EURATOM/UKAEA Fusion Association, Culham Science Centre, Abingdon, OX14 3DB, UK
[5] Max Planck IPP, Garching, Germany
[6] Institute of Plasma Physics and Laser Microfusion, EURATOM/IPPLM Association, Warsaw, Poland
[7] JET-EFDA, Culham Science Centre, Abingdon, OX14 3DB, UK

E-mail: roberto.cesario@enea.it

Received 23 August 2012, in final form 23 January 2013
Published 1 March 2013
Online at stacks.iop.org/PPCF/55/045005

Abstract
In this paper, we discuss the phenomena that link particle recycling from the vessel walls in the L-mode during discharge start-up and the core confinement in the H-mode during the subsequent main heating phase. We consider available data of JET experiments that aimed at approaching fully non-inductive ITER-relevant steady-state conditions and show that the high electron temperature produced at the edge by a low recycling during start-up tends to favour the build-up of high normalized β (β_N) regimes in the H-mode, the confinement being improved in a large plasma volume. To provide an insight into this complex phenomenon we have modelled the relation between particle recycling in the scrape-off layer and the evolution of plasma transport, plasma current density and shear as well as the stability properties for such experimental conditions. The results confirm the existence of a link between the confinement in the H-mode phase and the values at the edge of electron temperature, bootstrap current density and local magnetic shear during start-up. Such a link could favour these regimes to be self-sustained in time.

(Some figures may appear in colour only in the online journal)

1. Introduction

Full control of the plasma current profile represents a major objective for the progress of thermonuclear fusion research based on the tokamak concept [1], towards a steady-state (SS) energy source. In order to improve stability and confinement, it would be necessary to optimize the plasma current profile evolution [2–4]. In this context, utilizing lower hybrid current drive (LHCD) [5] has led to significant progress on JET by producing long-lasting transport barriers (TBs) with a relatively large radial position (at $\rho \simeq 0.6$–0.7, where ρ is the normalized toroidal flux coordinate) [6–8]. In these experiments, a plasma shape with low triangularity ($\delta \simeq 0.2$), plasma current (I_P) of 1.5 MA, toroidal magnetic field (B_T) of 3.45 T, safety factor at the edge (q_{95}) of about 8 were used. An H-mode was produced by externally launched power provided by neutral beam (NB) and ion cyclotron resonant heating (ICRH), applied after the end of the plasma current ramp-up (prelude phase). The lower hybrid (LH) power was applied both in the prelude and in combination with the main heating power. The cause of

[8] See the appendix of Romanelli F *et al* 2008 *Proc. 22nd Int. Fusion Energy Conf. 2008 (Geneva, Switzerland, 2008)* (Vienna: IAEA).

the observed TBs was identified as the low magnetic shear produced by LHCD power externally coupled during the H-mode phase [8]. In order to develop SS regimes at high normalized $\beta(\beta_N)$, a plasma with high triangularity ($\delta \simeq 0.4$) was used in experiments of JET at $I_P = 1.5$ MA, $B_T = 3.45$ T, $q_{95} \sim 7$–7.5, which obtained TBs with a larger radial size ($\rho \simeq 0.8$) yielding $H_{89} \simeq 2.0$, and normalized beta $\beta_N \sim 2$ [9].

More recently, experiments aimed at developing ITER-relevant SS regimes at high β_N with a lower $q_{95}(\simeq 5)$ were performed on JET [10, 11]. A plasma configuration of high triangularity ($\delta \simeq 0.4$) was used, with values of plasma current of 1.5 MA or 1.8 MA, and toroidal magnetic field of, respectively, 2.3 T or 2.7 T. The latter values of I_P and B_T were used in order to favour the deposition of the ICRH power in the core but with the same q_{95}. The line-averaged density at the beginning of the main heating phase was about 4×10^{19} m^{-3}. Consequently, an improved confinement up to $\beta_N \sim 3$ was obtained.

In performing these experiments [10, 11], the use of different gas fuelling waveforms in the prelude has allowed the assessment of different particle recycling from the vessel walls on confinement in H-mode. The possible occurrence of such an effect was indicated by data from previous campaigns [8, 14, 15]. All experiments considered in the paper belong to a homogeneous group of discharges performed in the same plasma configuration, which were aimed at developing SS ITER-relevant scenarios at high β_N in plasmas with high triangularity and $q_{95} \simeq 5$. We consider, in section 2, the subgroup of discharges performed with rigorously matched plasma density and the same timing of the main heating power, in order to enable detection of the effect of the initial level of recycling on confinement performance. The measure of the recycling level is obtained by the average of the spectroscopy diagnostic signals available for detecting the Dα emission. The emission is proportional to the density of neutrals available for charge exchange in the scrape-off layer (SOL). In the following, we refer to 'edge' as 'SOL', and 'periphery' as the radial layer of the plasma column within normalized minor radius $r/a \approx 1$–0.8. The β_N performance occurring during the main heating phase was linked to the recycling level measured before the switch-on of the main heating power. No systematic change in the recycling level occurred, instead, during the main heating phase.

The obtained results suggest reconsidering previous experiments and their modelling in a new light. We thus compare, in section 3, further discharges with the aim of focusing on a larger variety of change of prelude conditions, which have been produced by LH power or by a slightly different amount of gas fuelling. The goal of this search is to possess the key parameter(s) that determines initial conditions useful for producing a period of sustained high β_N during H-mode.

In this paper, we show the results of modelling of current density profile evolution, transport and stability supporting the hypothesis that the observed link between the initial condition of recycling and confinement performance should be the effect of the current drive and magnetic shear on confinement and stability, favoured by a higher edge temperature that is produced by a lower recycling.

The paper is organized as follows: section 2 shows the statistics that demonstrates, for given conditions of experiments on JET aimed at developing ITER-relevant SS regimes, the link between the initial condition of recycling and β_N performance during the H-mode phase; section 3 focuses on different conditions of prelude of experiments aimed at producing a high-β_N phase in developing SS scenarios; section 4 shows modelling results linking the particle recycling to kinetic profiles in the SOL; section 5 summarizes modelling results of current drive, transport, global stability and microinstability, and contains an hypothesis formulated for interpreting the phenomenology discussed in section 2; section 6 proposes an interpretation of the observed phenomenology, and section 7 is dedicated to comments and conclusions.

2. Phenomenology of recycling in the L-mode phase and confinement during the H-mode phase

The link between particle recycling from the vessel walls in the L-mode phase and confinement in H-mode is shown here as a result of a phenomenology occurring in experiments of JET aimed at developing ITER-relevant SS scenarios at high β_N [10, 11]. This phenomenology was obtained by statistics carried out on a wide group of plasma discharges performed with the same operating parameters (plasma configuration with high triangularity $\delta \simeq 0.4$, $I_P = 1.8$ MA, $B_T = 2.7$, $q_{95} \simeq 5$, and line-averaged density at the beginning of the main heating phase of about 4×10^{19} m^{-3}) with the exception, for some of them, of using a different gas fuelling waveform in the prelude which, however, was set to maintain the same density value for the plasma used as the target of the main heating power. Since the considered subgroup of homogeneous experiments (performed in the last four experimental sessions that concluded the operations of JET in carbon wall) was aimed at maximizing the main heating power for confinement improvement, a wide number of very similar plasma discharges was performed, which resulted useful indeed for the statistics in this work. This study is aimed, indeed, at assessing the role of small, but possibly significant, changes in the initial recycling condition (i.e. occurring just before the main heating power switch-on time) on confinement performance occurring in H-mode.

The monitored change in recycling was due to (i) the two different gas fuelling waveforms in the L-mode (prelude) phase, (ii) minor changes in gas fuelling that were automatically imposed by the feedback system for maintaining, shot by shot, the same target density. The operation with less gas fuelling before switch-on of the NB power is referred to as the *early gas fuelling overshoot*. This technique consists in setting the gas level with values markedly higher (up to about a factor two) with respect to the standard gas fuelling waveform in the early prelude (in the time window $t \approx 1.0$–2.0 s), and less gas (up to about 50%) in the late prelude phase, from $t \approx 3.0$ s up tot^-_{NB}, where t^-_{NB} is the time point just before the NB switch-on. The gas levels are set with the constraint of obtaining plasma targets of the NB power with the same density (4×10^{19} m^{-3}). This technique

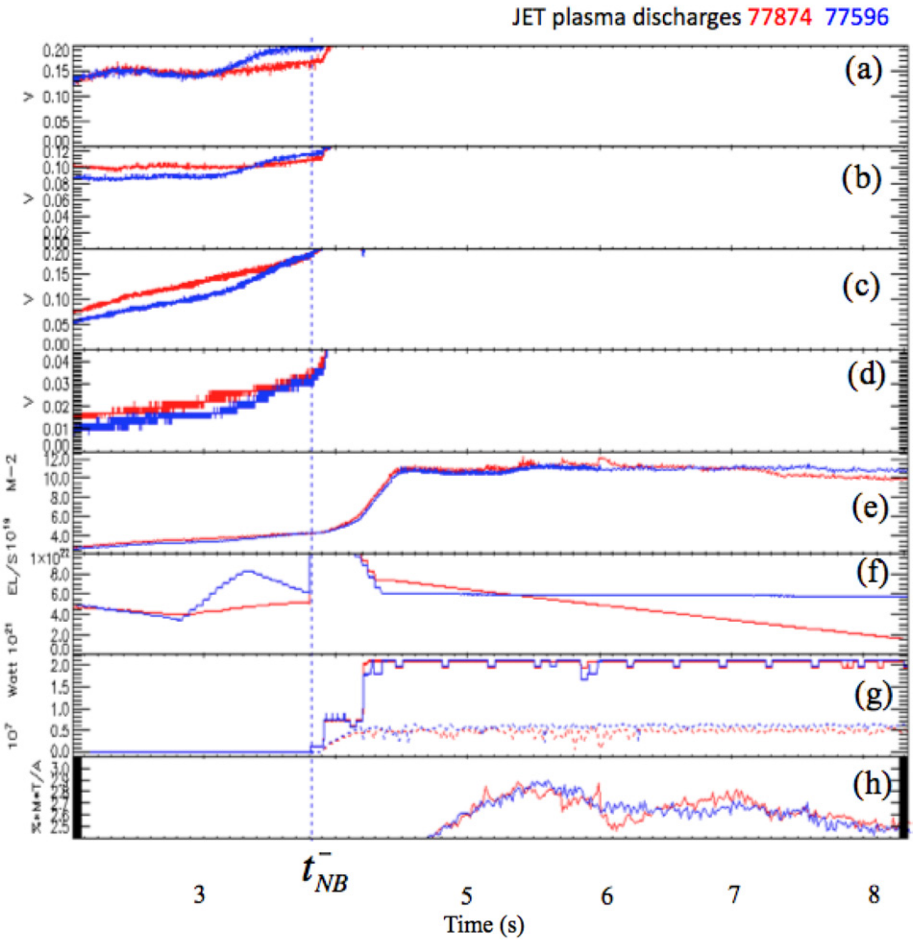

Figure 1. Time traces of some parameters of two discharges of JET aimed at developing ITER-relevant SS scenarios. Plasma parameters: $I_P = 1.8$ MA, $B_T = 2.7$ T, $q_{95} \simeq 5$, plasma shaped at high δ ($\simeq 0.4$): discharge 77874 (red lines), discharge 77596 (blue lines). Dα signals during late L-mode phase from the main vessel in the (*a*) horizontal and (*b*) vertical lines of sight, and divertor from the lines of sight on the (*c*) low-field side and (*d*) high-field side. (*e*) Line-averaged plasma density, (*f*) gas fuelling waveforms, (*g*) NB (continuous lines) and ICRH power (dotted lines), (*h*) normalized β (β_N).

was aimed at preparing plasma targets of the main heating power with a lower recycling with a consequent possible effect on confinement, as suggested by previous experiments [8, 14, 15].

In order to assess the evolution of recycling, the available data of the spectroscopy diagnostic channels that monitor the Dα emission were considered, along different lines of sight of the main chamber and divertor. Namely, the signals from the horizontal and vertical lines of sight of the main vessel, and from the divertor, respectively, in the low- and high-field sides were considered [16]. Focusing on the initial condition of recycling, in all discharges, the evolution of the Dα signal in the L-mode phase and β_N during H-mode was monitored. The conditions of the analysis are displayed in figure 1, which shows the time evolution of the relevant parameters of a couple of discharges (#77874 and #77596) performed, respectively, using or not the early gas fuelling overshoot technique.

Figure 1(*f*) shows the two different gas waveforms used in the late prelude. The statistics considers the average of the Dα signal levels kept at the time t^-_{NB}. The Dα levels during the main heating phase (not displayed in figures 1(*a*)–(*d*)) do not exhibit systematic differences in discharges compared in figure 1, as well as in all experiments considered for the statistics.

In most discharges, the maximum β_N occurs quite soon after the start of the main heating phase, see figure 1(*h*). However, since the experiments were aimed at developing scenarios towards the SS, we focused on monitoring the relative maximum β_N occurring later (2.5–3.5 s) after the time t^-_{NB}. Therefore, for discharges that exhibit a sufficiently sustained high-β_N phase (more than 1 s, i.e. several confinement times), β_{N_max} is considered within the time window $t = 6.5$–7.5 s. This choice enables making a possible link between edge physics in L-mode and the behaviour of the H-mode well after its formation more evident. The data analysis was performed considering the available data of all comparable discharges. The exact power level (within 0.5%) was considered in the relevant time window for measuring the occurring changes in maximum β_N (of the order of several per cent). In figure 1, discharge 77874 shows a β_N value slightly higher (of 4%) and more sustained in time than discharge 77596, figure 1(*h*). This trend linking lower initial recycling to a slightly confinement improvement occurred in all comparable discharges. The systematic occurrence of both β_{N_max} and sustainment of a high β_N values was monitored.

Both results of β_N and sustainment were considered important. The occurring of relatively low difference in β_N

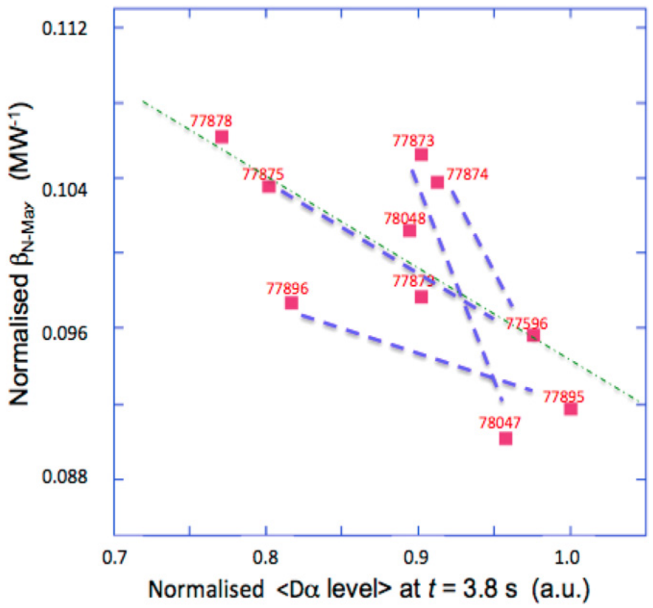

Figure 2. The maximum β_N (β_{N_max}) normalized to the main heating power and kept in a time window from 2.5 to 3.5 s after the main heating power switch-on time point is plotted versus the average of the available Dα signals, kept at the time t^-_{NB}. The operating main heating power is in the range 25–30 MW. The dashed segments link cases with matched main heating power (within 5%). The green line indicates the averaged trend.

should be, however, taken into account considering that only small changes in the operating conditions occurred in these experiments. The statistics is shown in figure 2.

The trend of the maximum β_N (normalized to the main heating power) monitored in the late H-mode phase is plotted against the average of the Dα signal levels measured at the time point t^-_{NB}. The displayed dashed segments link together cases with matched values of the main heating power (within 5%), which however does not change substantially in other cases (within 25%, from 25 to 34 MW). The most relevant outcome of figure 2 would consist in the amount of 100% of coincident cases linking a lower initial recycling to a higher maximum β_N. In particular, during the experiments, both discharges 77875 and 77895 of figure 2 obtained the highest β_N ($\simeq$ 3), but the former had a main heating power (27 MW) less than the latter (34 MW) and an initial recycling slightly lower (of 5%).

Therefore, for the considered conditions of experiment, a lower initial recycling occurring at the end of the prelude is linked to a higher β_N in the late H-mode phase. More specifically, a marked reduction in the initial Dα level ($\sim$30%) would produce a significant increase in β_N ($\sim$ 15%, see the green line in figure 2).

In order to help one understand the phenomenology shown by figure 2, the results of modelling of the SOL will be presented in the next section 4. This analysis was performed considering the data (I_P,B_T, input power and plasma density at the separatrix) of a discharge (77895) representative of the experiments considered for the statistics. The analysis showed that the lower recycling corresponds to a higher temperature in the SOL, consistent with [19].

However, in discharges of figure 2, the conditions in the prelude and the consequent changes in confinement performances (in terms of sustainment of the high-β_N phase) did not change by an amount sufficient for illuminating the mechanism at the base of the observed phenomenology.

We thus consider in the next section further data of similar experiments performed with more marked differences in the initial conditions, not necessarily of recycling but also of q-profile, produced by means of LHCD as well as different gas fuelling in the prelude. Consequently, these experiments obtained more marked differences in the evolution of the confinement performances in H-mode, which will help one to understand the related phenomenology by modelling.

We would mention the recent experiments of JET, aimed at improving confinement in the hybrid scenario [17] under the ITER-like wall condition, showing that operations exhibiting a lower recycling in the prelude also have a higher electron temperature at the plasma periphery, as well as an improved confinement in agreement with the trend appearing in figure 2. During the experiment, the following operating parameters were used: plasma configuration of high triangularity $\delta \simeq 0.4$, $I_P = 1.7$ MA and $B_T = 2.3$ T (corresponding to $q_{95}$of about 10% lower than in the considered experiments for SS scenario), $P_{NB} = 23$ MW, line-averaged density at the beginning of the main heating phase of about 4×10^{19} m^{-3} (as in the considered experiments for SS scenario). Moreover, in a discharge (83520), a transiently lower plasma volume (of about 25%) was tested in the prelude, then restored to the nominal value (of the reference discharge 83521) just before starting the main heating phase. As a consequence of the larger plasma–wall clearance and, hence, due to weaker plasma–wall interaction than in the reference discharge, the prelude of discharge 83520 exhibited a markedly lower recycling (of about 30%). For this discharge, the electron temperature at the periphery (r/a = 1–0.8), measured by a high-resolution Thomson scattering diagnostic (HRTS), was slightly higher (from 100% to 25%, respectively) than that in the reference discharge, well outside the experiment uncertainties and consistent with the behaviour of low recycling documented in [19] (and with the aforementioned modelling results, which will be shown in section 4). Regarding confinement performance, in the discharge with lower recycling, β_N ($\approx$ 3.0) occurring in H-mode was markedly higher (of about 15%) with respect to the reference discharge ($\beta_N \approx 2.6$). The result linking lower initial recycling and higher β_N in H-mode is in agreement with the trend shown in the statistics of figure 2. This would thus represent a behaviour more general, which would not apply only to experiments aimed at developing SS scenarios in carbon wall with $q_{95} \simeq 5$.

3. Prelude conditions and the high-β_N phase

The link of the initial condition of recycling and confinement performance in H-mode, shown by the phenomenology described in the previous section, has suggested exploring the role of the prelude operating conditions in determining high-β_N phase performances in more depth. The role of q-profile in the prelude in determining the evolution of the current profile and, consequently, stability and confinement in H-mode [18] is well assessed. In this section, we discuss

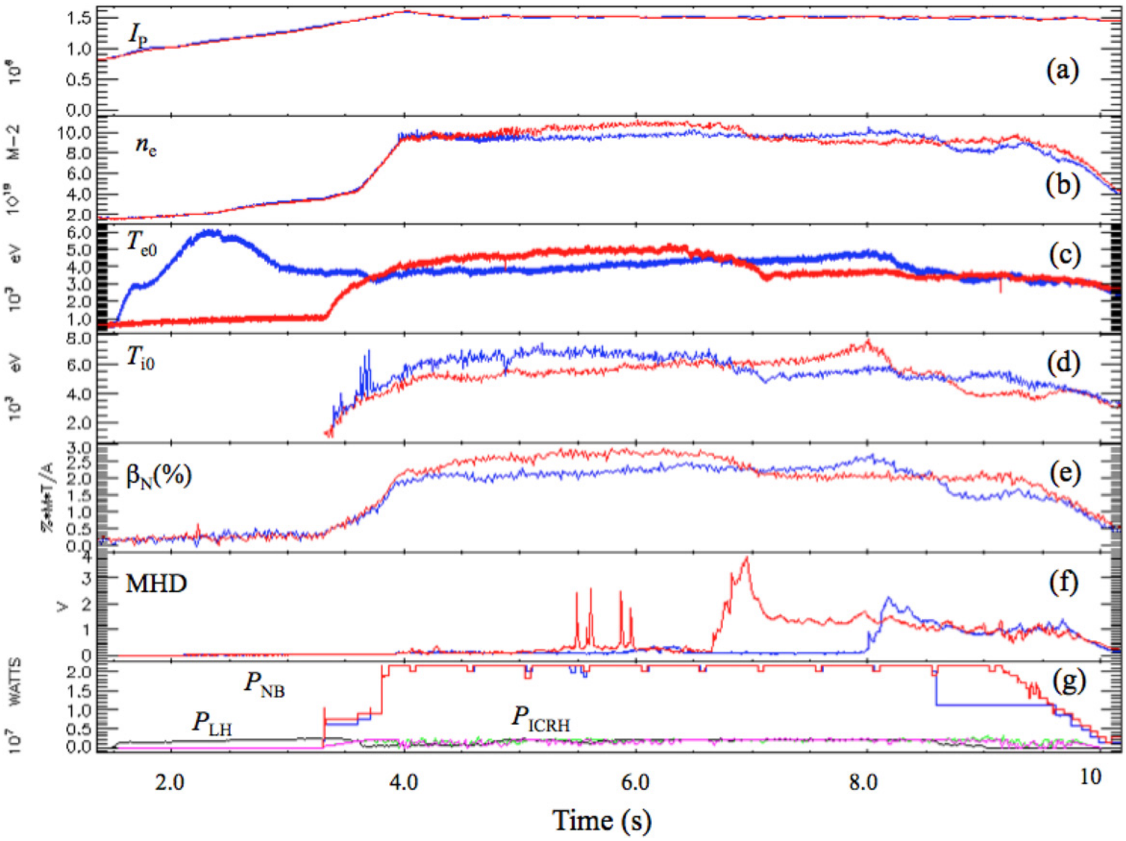

Figure 3. Time traces of the main parameters of two experiments considered in the modelling: discharges 70069 (red lines), 70068 (blue lines): (*a*) plasma current, (*b*) line-averaged plasma density, central temperature of (*c*) electrons (from ECE), (*d*) ions, (*e*) β_N, (*f*) MHD (mode 2,1), (*g*) NB power, ICRH power: discharge 70069 (magenta line), discharge 70068 (green line), LH power only in discharge 70068 (black line).

on experiments representative of the attempts for achieving confinement performance in H-mode by optimizing the q-profile in the prelude and utilizing different conditions of current drive produced by LH power. This goal was not achieved by changing the LH power parameters (power level, $n_\parallel$), but only by less gas fuelling in the prelude, which produced lower density, higher temperature, in the core and at the periphery, and lower recycling ($n_\parallel$ is the refractive index component in the direction parallel to the confinement magnetic field).

We focus here on three reference discharges performed with the same operating parameters as those considered in section 2 (plasma configuration of high triangularity $\delta \simeq 0.4$, $q_{95} \simeq 5$, and line-averaged density at the beginning of the main heating phase of about $4 \times 10^{19}\,\mathrm{m}^{-3}$), but different conditions of prelude, consisting in utilizing, or not, LH power, or using different gas fuelling waveforms. The time traces of the main plasma parameters are shown in figures 3 and 4, which compare the cases of, respectively, purely ohmic and LH preludes (discharges 70069 and 70068), and two different regimes of recycling and density obtained by different levels of gas, for the same case of an LH prelude (discharges 72495 and 70068).

The LH power was used for driving a non-inductive current during the prelude, in order to produce a different q-profile at the beginning of the main heating phase of discharge 70068 with respect to discharge 70069 of figure 3. This figure shows that only discharge 70069 performed with a purely ohmic prelude exhibits a high-β_N phase (figure 3(*e*)). This period lasts for about 2 s (ten confinement times) and terminates at the onset of a strong MHD event (mode 2/1), figure 3(*f*). Discharge 70068 begins a high-β_N phase late similar to shot 70069 but it is cut short by MHD.

It is worth noting that the evolution of kinetic profiles of discharge 70069 of figure 3 and those of discharges considered for the statistics of section 2 are similar. Also the latter experiments were performed, indeed, with a purely ohmic prelude, in the same plasma configuration, with the same value of q_{95} and with the same density as for discharges considered in the statistics of figure 2. The kinetic profiles are provided by the diagnostics of core and edge LIDAR (for plasma density and electron temperature) and by electron cyclotron emission (ECE, for electron temperature), and charge exchange for ion temperature. In particular, the data from the core and edge LIDAR diagnostics allow determining the kinetic profiles necessary for performing the modelling, which will be shown in section 5, of current drive, transport and stability that includes plasma conditions at large radii. Therefore, the kinetic profiles and equilibrium-reconstructed data of discharge 70069 represent a typical behaviour of the high-β_N plasmas considered in the paper. These data will be used as input data for the modelling analysis shown in section 5.

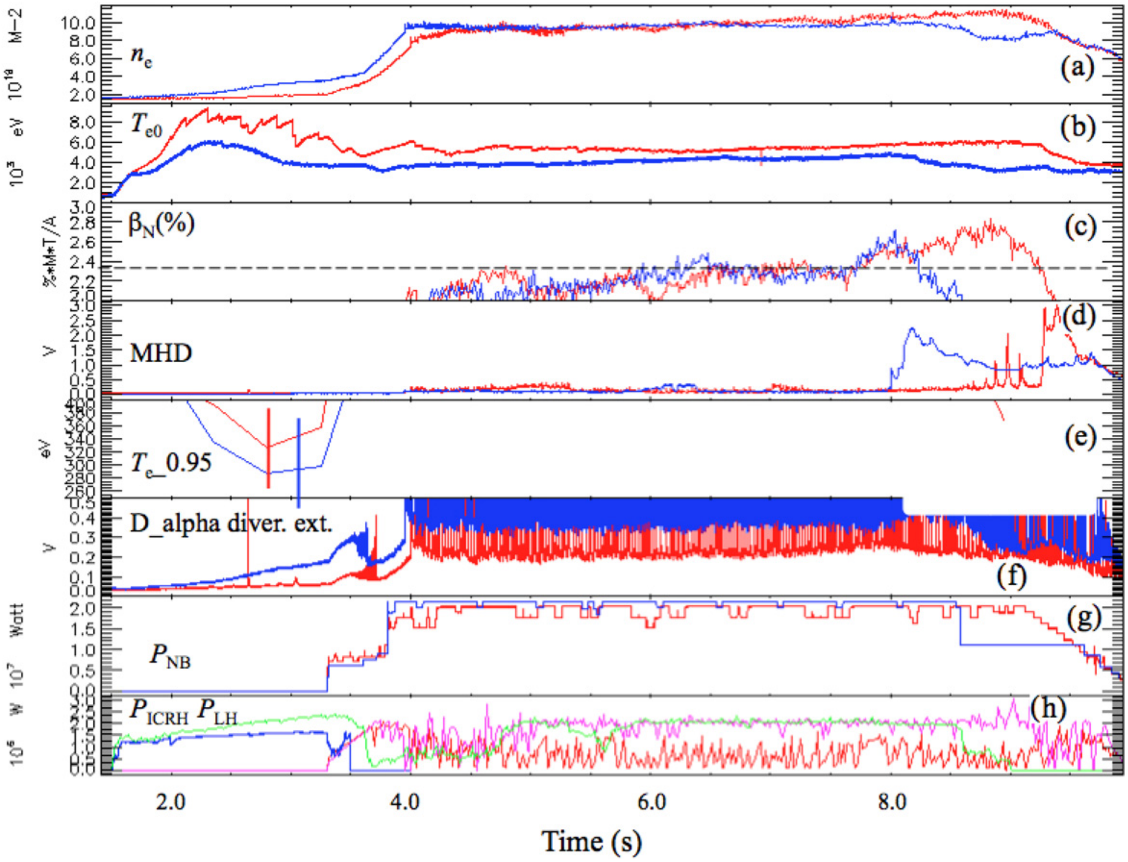

Figure 4. Time traces of the main parameters of discharges 72595 (red lines in all boxes but in (*h*)), 70068 (blue lines in all boxes but in (*h*)): (*a*) line-averaged plasma density, (*b*) electron temperature, (*c*) normalized beta, (*d*) MHD (2/1) monitor, (*e*) electron temperature at the periphery ($r/a \approx 0.9$ interpolated from LIDAR and edge-LIDAR), (*f*) Dα level from the divertor (low-field side line of sight), (*g*) NB power, (*h*) LH power: discharge 72595 (blue line), discharge 70068 (green line), ICRH power: discharge 72595 (red line), discharge 70068 (magenta line).

An extensive search was performed for testing possible improvement of performance in H-mode by means of an LH prelude. Utilizing the same operating parameters of discharge 70068 of figure 3, the effect of different coupled LH power levels and $n_{\parallel}$ antenna spectra was tested. Consequently, the main heating phase was characterized, however, by the absence of a high-β_N phase.

Following previous results suggesting that a lower recycling in the prelude would help in the formation of improved confinement during H-mode [8, 14, 15], an experiment was performed using the same operating parameters as for discharge 70068 of figure 3, but with slightly less gas fuelled in the prelude. This experiment produced discharge 72595 of figure 4. Due to the less gas fuelled in the prelude, this discharge has, at the switch-on time of the main heating power ($t_{NB}^{-} \approx 3.3$ s, see figure 4(*e*)), a lower density (figure 4(*a*)), higher electron temperature (figure 4(*b*)) and markedly lower Dα level (figure 4(*f*)) than the reference discharge (70068). A lower Dα level occurs in the prelude as well as throughout the H-mode phase for shot 72595. It will be shown in section 4 that this behaviour of lower recycling is consistent with higher temperature occurring at the plasma edge. The occurrence of higher temperature in the prelude at large radii for shot 72595 is documented by figure 4(*e*). During H-mode (e.g. at $t = 5$ s), the electron temperature at large radii is higher in shot 72595, by about 40% at $r/a \approx 0.9$ (1380 eV in shot 72595 against 970 eV in shot 70068), and by about 20% at $r/a \approx 0.8$ (1750 eV in shot 72595 against 1420 eV in shot 70068), thus justifying the Dα level behaviour of figure 4(*f*).

The less gas in the prelude did not produce significant delay (∼100 ms) in the L–H mode transition time: consequently, a desired ELMy H-mode phase was regularly produced [9], see figure 4(*f*). Therefore, the confinement performance of discharges of figure 4 can be compared. The phase with a high β_N (in the range 2.5–2.8, figure 4(*c*)) occurs in discharge 72595, despite the fact that the NB power is 5% less than that in the reference discharge (70068). The high β_N (>2.3 i.e. the level during the H-mode phase without confinement improvement) occurs in the late H-mode phase (for $t \geqslant 8.2$ s) and persists for more than 1 s for the entire time in which the NB power flat-top is maintained, see figure 6(*g*). In fact, at the NB switch-off time point ($t = 9.2$ s), β_N is about 2.5 and strong MHD event occurs only (at $t = 9.3$ s) when the NB power is falling off.

Regarding the use of LH power coupled during the main heating phase, this operation did not ever produce, in the considered plasma configuration, current drive effects in the core, as LH waves were fully deposited at the edge by the parasitic effect [12]. This result was the consequence of the relatively high plasma density at the edge and periphery of the main plasma that typically occurs in the main heating phase of plasmas shaped at high triangularity. Unfortunately, the method assessed on FTU (Frascati Tokamak Upgrade) for enabling the occurrence of LH effects also at markedly higher densities [13] was still not available at the time of the considered experiments of JET. However, thanks to the successful result of a high-β_N phase obtained also with an LH prelude in discharge 72595 of figure 4, both the LH as well as the ohmic preludes can be considered tools useful for producing a high-β_N phase for developing SS scenarios.

The problem now is to interpret the obtained results. Namely, it should be understood why, in the considered scenario, a high-β_N phase is produced with a purely ohmic prelude but not with an LH prelude, and why this problem has been overcome operating, instead, with less gas in the prelude, producing lower density, higher temperature and lower recycling. Our aim is to individuate, by modelling performed on the basis of the results of the previous two sections, the relevant parameter(s) that, acting as the initial condition before the start of the main heating phase, allow building a sustained high-β_N phase. The modelling data shown in the next two sections are useful for trying to solve this problem and support the interpretation proposed in section 6.

4. Particle recycling from the vessel walls and temperature at the plasma edge

It is well assessed that by operating with a lower particle recycling from the vessel wall, a higher temperature occurs at the edge, as a consequence of the lower radiation loss from the plasma edge [19]. However, as an example of this effect, we present here available data of the modelling performed taking into account the parameters of a reference discharge (77895) considered in section 2.

Transport modelling is carried out by the EPIT code [20]. The transport along field lines is assumed to be classical and transport coefficients follow from the 21-moment Grad approximation [21, 22]. The radial transport is assumed to be anomalous with prescribed radial transport coefficients. All ion species have the same temperature T_i, which can be different from the electron temperature T_e. The dynamics of deuterium and impurity neutrals in the SOL is described by an analytical model, which accounts, in a self-consistent way, for recycling of plasma ions as well as for sputtering processes at the target plates. In the present analysis, the effect of impurities is neglected and only a deuterium plasma is considered. For the sake of simplicity, the analysis is performed in the slab geometry, neglecting the real curvilinear structure of the magnetic field in the SOL of the JET tokamak, meaning that $hx = hy = \sqrt{g} \equiv 1\sqrt{g}$ (hx and hy are metric coefficients). In order to account for the magnetic flux tube expansion in the divertor, we assume that the pitch angle changes in the divertor according to the following formula:

$$h_\theta(x) = \left(\frac{B_\theta}{B}\right)_{\text{separatrix}} \qquad \text{for} \qquad x < x_s \qquad (1)$$

where x_s is the poloidal position of the x-point.

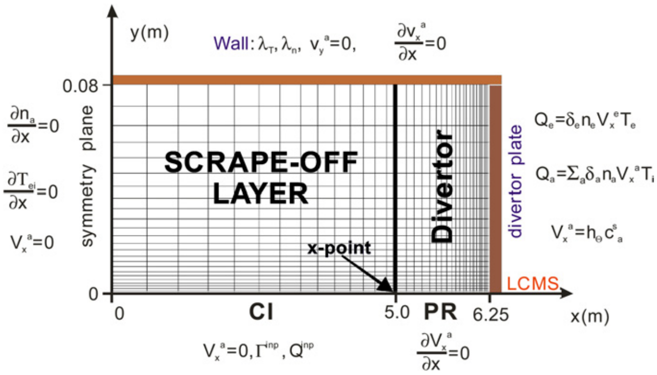

Figure 5. Computational mesh and boundary conditions.

We note that the geometrical effects related to the real structure of the JET SOL and divertor are of minor importance for the plasma conditions at the outer target plates considered in the paper. In fact, the energy transport along the field lines is the dominant physics mechanism, which is well described by the simple geometry, in particular, in view of simplifications of the neutral model.

We consider the data of discharge 77895: $I_P = 1.8$ MA, $B_T = 2.7$, power flowing to the SOL $P_{SOL} = 1.2$ MW and density at the separatrix 0.96×10^{19} m^{-3}. The anomalous radial transport is determined by the coefficients $D^i = 0.1$ m^2 s^{-1}, $\eta_y^i = 0.2 m_i n_i D^i$ and $\chi_y^e/n_e = 2.5\chi_y^i/n_e = 10D^i$. In all calculations, the input particle flux to the SOL $\Gamma_{inp} = 3 \times 10^{21}$ s^{-1}.

Boundary conditions used in our calculations are shown in figure 5 where the computational domain and the numerical mesh are also presented. At the core interface, constant input energy and particle fluxes as the boundary condition are specified. We assume that all radial gradients are zero at the interface with the private region (PR). Density and temperature decay lengths are used as boundary conditions at the wall. The Bohm condition is used at the divertor plate: the flow velocity at the plate equals to the poloidal projection of the sound speed: $v_{ix} = h_\Theta c_s$ and the energy fluxes are given by $q_{ex} = \delta_e n_e v_{ex} T_e$, $q_{ix} = \delta_i n_i v_{ix} T_i$, where c_s is the sound speed and the energy transmission factors δ_e and δ_i are calculated according to the Igitkhanov model [23].

In the case of deuterium, two groups of neutrals are considered: fast and slow neutrals ($N_D = N_{fD} + N_{sD}$). The profile of deuterium atoms is prescribed by a product of exponential functions:

$$N_D^{f,s}(x, y) = N_{f,s}^{\text{plate}} \mathrm{e}^{\frac{|x_{\text{plate}} - x|}{\lambda_x^{f,s}}} \mathrm{e}^{-\frac{(y_M - y)^2}{\lambda_y^{f,s}}} \qquad (2)$$

The deuterium neutral densities at the target plate depend on the recycling coefficient R:

$$\int_{\text{VOL}} N_D(x, y)\alpha_i^D(x, y) n_e(x, y)\,\mathrm{d}V = R \int_{\text{plate}} |n_i v_x^i|(x_{\text{plate}}, y)\,\mathrm{d}s \qquad (3)$$

where VOL is the volume of the boundary layer and R is an external parameter in the SOL model. It is assumed that the

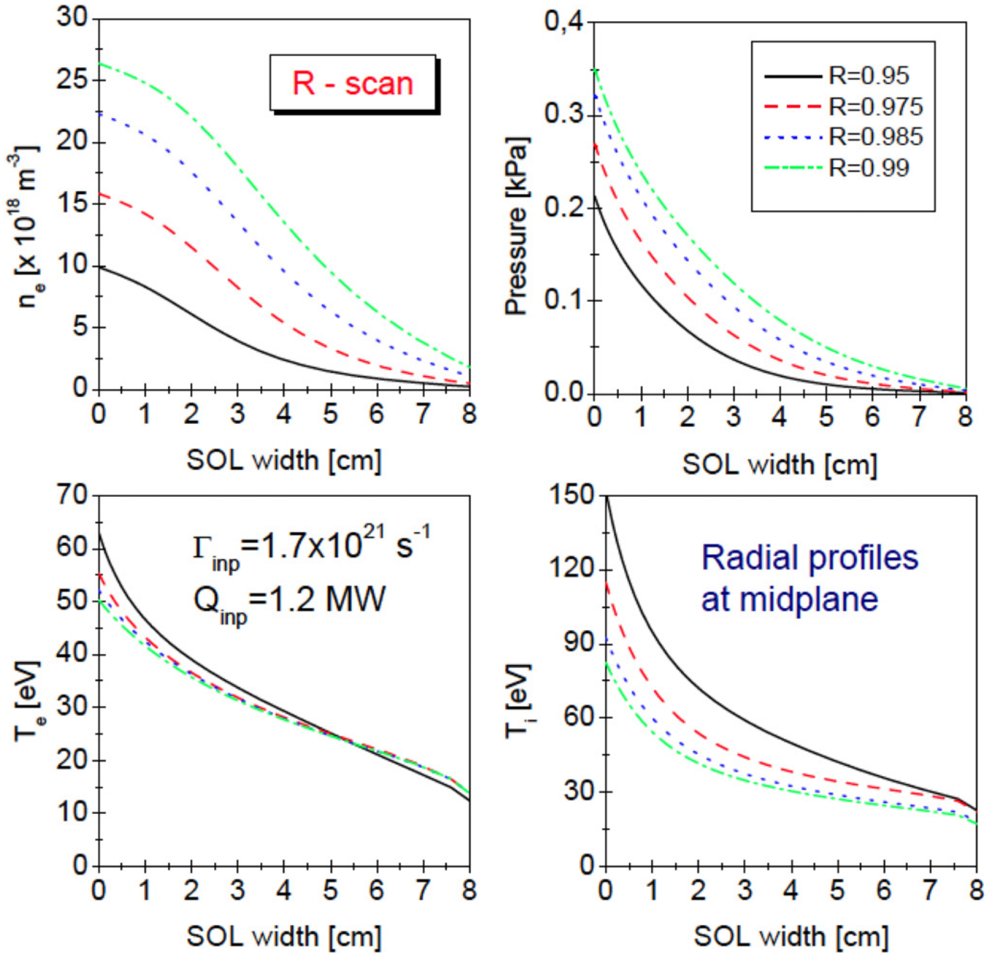

Figure 6. Radial plasma kinetic profiles in the SOL at the midplane for different recycling coefficients. Plasma parameters of discharge (77895) considered in section 2.

velocity of the neutrals is equal to the ion velocity for fast neutrals and it is equal to the thermal velocity in the case of slow neutrals.

The influence of the recycling coefficient on the plasma parameters in the SOL was investigated. The recycling coefficient was changed from $R_c = 0.95$ up to $R_c = 0.99$ and the corresponding changes in the total plasma flux to the target plate are $\Gamma_{plate} = 6 \times 10^{22}$ to 30×10^{22} s^{-1}. The results are summarized in figure 6.

It is evident that a higher plasma recycling leads to an increase in the plasma density and pressure and a reduction in the plasma temperature. This effect is relatively strong close to the divertor plate strike point. A decrease of about 25% in the recycling coefficient (R_c, from 0.975 to 0.950) corresponds to a decrease of 50% in the Dα radiation, $P_{rad-Da} \propto 1/(1 - R_c)$. The temperature profile in figure 6 shows that, for low recycling operation, the most marked enhancement of T_e is expected to occur in the deeper radial region of the SOL, i.e. at $\rho \sim 1$. The temperature at this layer will be referred to as T_{e_edge}. A decrease of 50% in the Dα radiation gives an increase of about 15% in T_{e_edge}. A similar result has been found considering data of experiments aimed at developing SS scenarios on JET with plasma configuration at low triangularity ($\delta \simeq 0.2$) and higher $q_{95}(\sim 8)$ [6–8].

5. Modelling of the plasma current profile evolution, transport and stability

In this section, we show modelling data that help one to understand the complex phenomenology shown in section 2, which connects the level of recycling occurring in the prelude phase, before the NB switch-on time, to the confinement performance in H-mode.

Available data of experiments showed, in section 3, that a high-β_N phase is successfully produced using a purely ohmic prelude. Moreover, by coupling LH power in the prelude for driving a non-inductive current, a high-β_N phase occurs provided that less gas fuelling is utilized, which produces, with respect to the reference discharge, slightly different initial conditions of lower density, higher temperature also at the edge and lower recycling. A lower recycling accompanies higher temperature at the edge and periphery, as assessed in section 4, section 2 and [19]. Our search considers the well-assessed role played by the prelude$q$-profile in determining the evolution of the current profile and, consequently, stability and confinement in H-mode [18]. Therefore, our search focuses on a mechanism that reasonably links together initial conditions of recycling and current density profile.

We summarize here the modelling results of the evolution of the radial profiles of current density, magnetic shear,

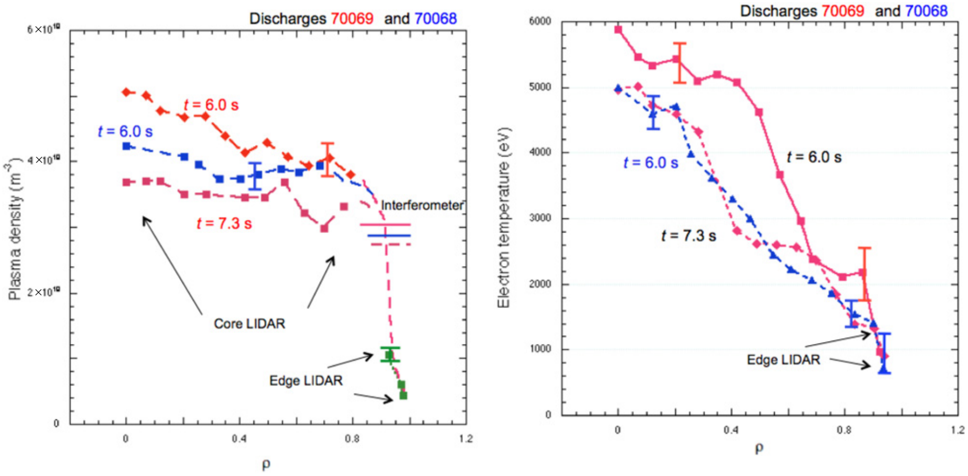

Figure 7. Electron plasma (*a*) density and (*b*) temperature profiles of experiments of figure 3. Discharge 70069 having a high-β_N phase: the profiles at $t = 6.0$ s are obtained by averaging the available data from $t = 5.5$ s and $t = 6.5$ s, and those at $t = 7.3$ s are obtained by averaging from $t = 6.8$ s to $t = 7.8$ s. Discharge 70068: the profiles at $t = 6.0$ s are obtained by data averaged from $t = 5.5$ s to $t = 6.5$ s.

transport and stability, taking into account the kinetic profiles of experiments shown in section 3, which exhibit or not a high-β_N phase, as a consequence of having used preludes, respectively, purely ohmic or with LHCD. For the same discharge (70069) with a purely ohmic prelude of figure 3, we compare the respective phases of standard H-mode and high β_N. In a further comparison, we consider the same time window relevant for the occurrence of the high-β_N phase in both discharges with different preludes of figure 3.

For these discharges, only discharge 70069 presents a high-β_N phase (figure 3(*e*)) that terminates at the onset of strong MHD event (mode 2/1), see figure 3(*f*). Due to the LH power coupled in the prelude phase, in discharge 70068, a target for the main heating power with deeply reversed q-profile is expected to occur, as a consequence of non-inductive current driven in the core. As discussed in section 3, discharge 70068 of figure 3 belongs to a series of experiments in which the achievement of high β_N was prevented by strong MHD event occurring very early. For this reason, before having obtained the new successful result with an LH prelude (in discharge 72595 of figure 4), the LH prelude was not considered a tool useful for producing well-confined and stable plasmas for developing the considered SS scenarios. We would thus try to understand why the LH prelude would not produce a suitable condition for confinement performance, in the operating condition of discharge 70068.

In order to model the evolution of the radial current density profile and perform transport analysis, the following approach was employed.

The model of neoclassical resistivity (NCLASS) and the Faraday equation included in the JETTO code [24] are used to determine the current diffusion in the plasma column by taking into account the kinetic profiles, the effective ion charge and the EFIT [25] equilibrium reconstructed using magnetic data. The used kinetic profiles occurring during the high-β_N phase (at $t = 6.0$ s) and after its termination (at $t = 7.0$ s) for discharge 70069, and during H-mode (at $t = 6.0$ s) for discharge 70068 are shown in figure 7.

The density profiles (figure 7(*a*)) are assumed to have the same steep gradient within the uncertainties of the two LIDAR and the interferometer diagnostic systems. This choice overestimates the gradient in case (discharge 70068) a slightly lower density is reached during the H-mode phase, thus allowing a more confident comparison of the j_{BS} profiles occurring in the compared experiments. For discharge 70069, during the high-β_N phase, a slightly higher pedestal density ($\sim$10%) occurs indeed, as shown in figure 7(*a*), while $T_{e-\text{periphery}}$ (at $\rho \sim 0.8$, figure 7(*b*)) is slightly higher (by about 20%) than after the high-β_N phase termination. After that time, $T_{e-\text{periphery}}$ is reduced to a value close to that occurring in discharge 70068 that does not present a high-β_N phase. A significant effect of the electron temperature at the periphery on locally enhancing j_{BS} for discharge 70069 is thus expected to occur, due to the contribution of the term in the relation [1]

$$j_{BS} \propto T\nabla n + 0.04\nabla T. \tag{4}$$

In the JETTO code, the complete expression of the bootstrap current is used [26]. Incidentally, an analysis of the current drive in experiments of [10,11] including discharge 70069 was also performed using the TRANSP code [27], but this work did not include the available data of plasma periphery as done instead in this paper (ρ0.9).

In case with LH power utilized in the experiment, the correspondent deposition profile is calculated with the LH$^{\text{star}}$ code, which includes the wave physics of the plasma edge and periphery [13, 28, 29].

The EFIT code also provides the current density profile in the very early phase of the discharge ($t \sim 1$ s), which is used as the initial condition for the JETTO simulation.

Figure 8 shows some results of plasma current profile evolution.

Figure 8(*a*) compares, for discharge 70069 of figure 3, the q-profile evolution during the H-mode phase modelled by JETTO with that provided by EFIT using magnetic input data constrained by motional Stark effect (MSE) measurements, and general agreement is found. Moreover, the q-profile

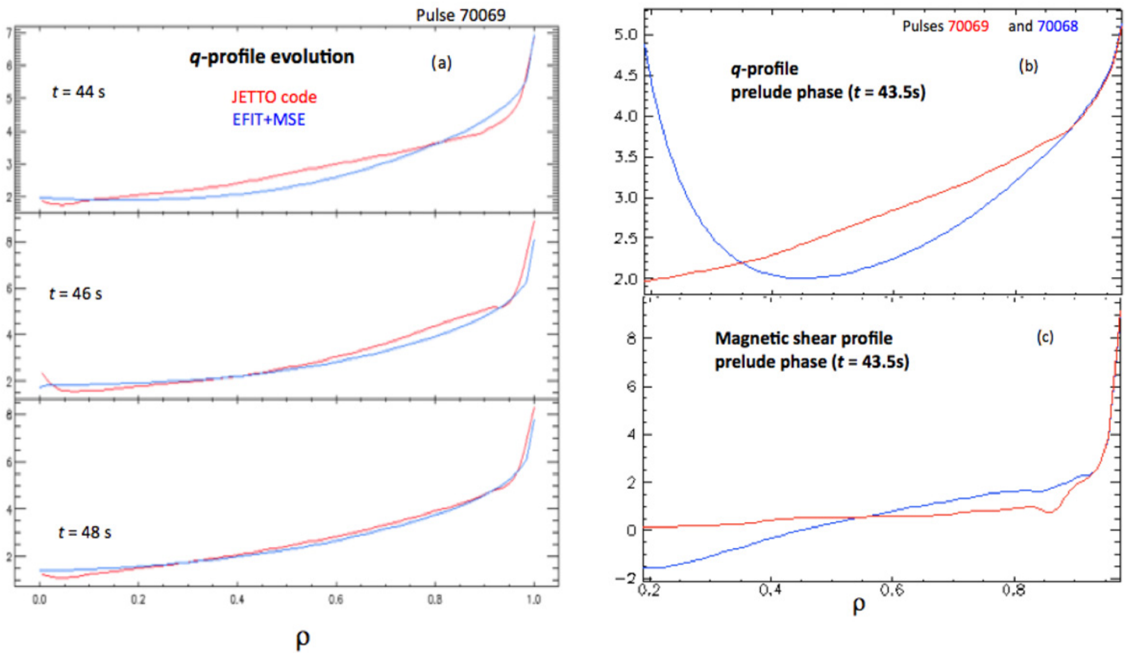

Figure 8. (*a*) q-profile evolution during the main heating phase at three different time points as obtained by the modelling of JETTO and compared with the available EFIT+MSE data measurements for the discharge 70069 of figure 3. (*b*) q and (*c*) s-profile in the prelude phases (at $t = 3.5$ s) of the discharge 70068 of figure 3.

modelled with JETTO shows a local flattening during the main heating phase ($t = 6.0$ s) at large radii ($\rho \approx 0.90$), which indicates the occurrence of a region of low magnetic shear. Conversely, a similar analysis performed for discharge 70068 of figure 3 shows that the flattening of the q-profile at large radii is much less pronounced than in the case of discharge 70069 (figure 8(*a*)), which indicates the occurrence of a higher local shear for discharge 70068. Unfortunately, the EFIT reconstruction method and MSE measurements used to determine the q-profile do not allow a precise determination of such a feature localized in this region of plasma. The used approach for modelling the q-profile evolution, which includes the available data of kinetic profiles at the plasma periphery, also provides a useful tool for properly considering, in the realistic context of the experiment, the local effects of the magnetic shear on transport.

For the same discharges of figure 3, the q- and shear profiles at a time point ($t = 3.5$ s) just after the main heating power switch-on are compared in figures 8(*b*) and (*c*). This comparison is useful for assessing the role of different initial conditions in the compared plasmas. For the case with an LH current drive prelude (discharge 70068) a deeply reversed q-profile is obtained, as expected, figure 8(*b*). Moreover, the magnetic shear at large radii in the prelude is markedly higher for shot 70068, see figure 8(*c*).

Therefore, as an important result, the plasma with an LH prelude represents a plasma target for the main heating power that is farer from the condition of low magnetic shear at large radii than that with a purely ohmic prelude. The shear at large radii ($s \approx 1.5$ at $\rho \approx 0.85$), figure 8(*c*), is markedly higher than that in the case with a purely ohmic prelude ($s \approx 0.6$ at $\rho \approx 0.85$), a consequence of the negative shear produced in the core. This undesired condition is related to the deeply reversed q-profile occurring in the case with an LH prelude, figure 8(*b*), as the LH current is mostly driven in the inner radial half of the plasma, due to the radially narrow T_e profile target ($T_{e0} \approx 4.5$ keV, $T_e \approx 2$ keV at $\rho \approx 0.35$) occurring in the prelude. The LH current density calculated with the LH$^{\text{star}}$ code, considering the plasma parameters of discharge 70068, is $j_{\text{LHpeak}} 5 \times 10^6$ m^{-3} at $\rho \approx 0.35$, and $j_{\text{LH}} \approx 2 \times 10^6$ m^{-3} at $\rho \approx 0.40$.

Transport analysis was performed considering the parameters of discharge 70069 of figure 3. The two phases of H-mode are compared, respectively, during (at 5.5–6.0 s) and after (at 7.3–7.8 s) the high-β_N phase, see figure 3(*e*). The radial profiles of the electron and ion thermal diffusivities are shown in figure 9.

During the high-β_N phase, the electron conductivity is markedly lower (more than a factor two) in the whole radial region $\rho 0.6$, and slightly lower (30%) more externally (up to $\rho \approx 0.8$). The ion conductivity presents less pronounced differences: it is 40% lower for $\rho 0.5$ and 20% for $\rho 0.8$. Consequently, the high-β_N phase is characterized by a radially large TB.

We now show the radial profiles of the plasma current density and magnetic shear for the discharge 70069 of figure 3 with a high-β_N phase. Figure 10 displays the contributions of the NB power and the bootstrap effect at two different time points, respectively, before (at 6.0 s) and after (at 7.3 s) the high-β_N phase termination. The magnetic shear radial profiles are shown in figure 10(*b*) in a way useful for evidencing large plasma radii. Two couples of time points are considered, respectively, before (at 5.0 s and 6.0 s) and after (at 7.3 s and 8.0 s) the high-β_N phase termination.

A low shear ($s \approx 0.2 \pm 0.02$) thus occurs at large radii ($\rho \approx 0.92 \pm 0.02$) during the high-$\beta_N$ phase of the considered AT discharge.

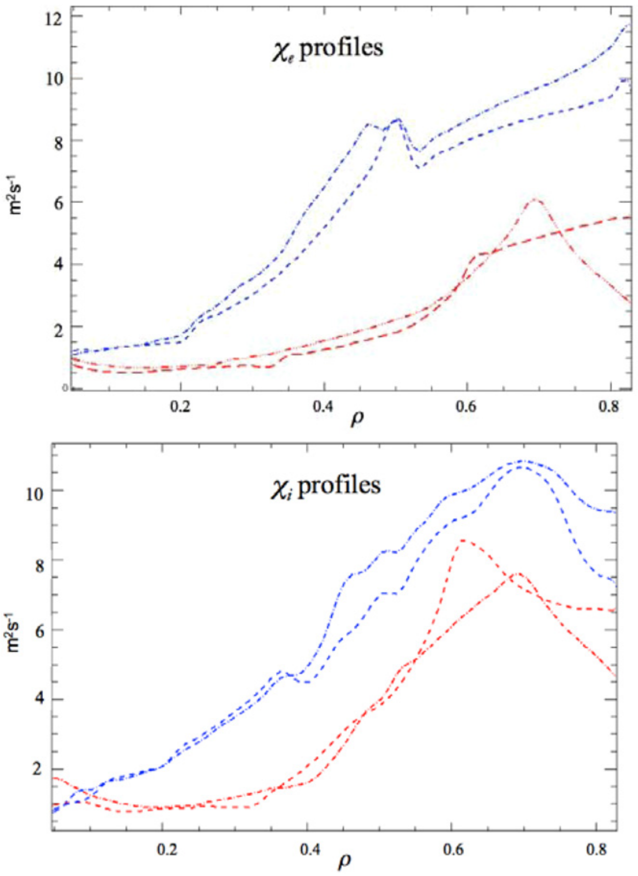

Figure 9. Thermal diffusivity at different time points of discharge 70069 of figure 3. During the high-β_N phase, the couples of (red) curves displayed mostly in the lower box region refer to $t = 5.5$ s (dashes) and $t = 6.0$ s (dot-dashes). After the termination of the β_N phase, the couples of (blue) curves displayed in the upper box region refer to $t = 7.3$ s (dashes) and $t = 7.8$ s (dotted–dashed).

A stability analysis is carried out using the ideal MHD code MISHKA-1 [30] considering the main heating phase of discharges of figure 10. The equilibria for the same plasma discharge of figure 10 are reconstructed from the current density and pressure profiles derived from JETTO simulations. These profiles, together with the fixed boundary shape of the last closed flux surface, are supplied to the HELENA code [31], which produce the static equilibrium employed by MISHKA-1. The plasma is found to be stable to infinite-n ballooning modes at the low magnetic shear generated by the strong bootstrap current, see figure 10(a). However, the plasma discharge (70069) with a high-β_N phase has a bigger margin of stability minimum shear at the plasma periphery ($\Delta s_{\min} \approx 4.0$, $\beta_{N\max} \approx 2.8$ for discharge 70069) than the plasma with lower β_N ($\Delta s_{\min} \approx 2.3$, $\beta_{N\max} \approx 2.6$ for discharge 70068). $\Delta s_{\min}$ is the minimum distance in magnetic shear between the experimental plasma and the stability boundary.

Considering discharges of figure 4, a stability analysis of the plasma edge during the prelude is performed using the GENE code [32]. For the parameters of the discharge (70068) with higher density and lower temperature, during the L-mode phase unstable ETG modes are predicted to be present, while they are much weaker (but still slightly unstable) for the compared discharge (72595). Simulations aimed at assessing the non-linear behaviour of turbulence are in progress and full results will be presented in a dedicated work.

It is worth noting that the modelling of the current drive was performed considering several time points (about ten) during and after the collapse of the high-β_N phase. Consequently, the relatively high bootstrap current fraction and low shear of discharge 70069 of figure 3 is representative of the behaviour of the high-β_N phase since its build-up (at $t \approx 4$ s), as kinetic profiles at the periphery are similar to those displayed in figure 7.

These circumstances suggest that the initial condition of lower shear (figure 8(c)) would favour the build-up of an improved confinement phase that, in turn, produces higher temperature at the periphery since the beginning of the main heating phase. In an analogous way, initial conditions of low recycling, favouring the occurrence of higher temperature at the edge and periphery, would also help the build-up of a higher bootstrap current fraction and the initial condition of low shear at large radii.

In the next section, we propose some ideas that help in understanding the described phenomenology linking together initial conditions of low recycling, higher electron temperature at the edge and periphery (discussed in sections 2 and 4) and magnetic shear (discussed in the present section) to the build-up of improved confinement in H-mode.

6. Interpretation of the phenomenology

We propose an interpretation of the phenomenology discussed in sections 2 and 3, which shows that the initial conditions of kinetic profiles and magnetic shear at large radii are linked to the build-up of an improved confinement phase in H-mode. Due to the intrinsic complexity of the phenomenology, we could not give a fully exhaustive explanation but present some ideas that help one to understand the phenomenology and address a more complete search on the related matter.

The considered plasmas have an H-mode phase that starts just after the end of the current ramp-up when the current is not fully relaxed, as shown by the q-profile evolution of figure 8(a). The high-β_N regimes are accompanied by radial profiles that present, at the periphery ($\rho \sim 0.8$–0.9), a relatively high electron temperature and bootstrap current density, and low magnetic shear ($s \approx 0$). The high bootstrap current fraction and low shear at large radii are representative of the behaviour of the high-β_N phase. The kinetic profiles displayed in figure 7 are typical of such plasmas. Moreover, the enhanced β_N period is favoured by operations that produce a lower recycling in the prelude, before the NB power switch-on time point, as demonstrated in section 2. As shown by experimental data in section 2, modelling results of section 4 and [19], low recycling regimes are characterized by a relatively high temperature at the plasma edge and periphery. Analysis of microinstability shows that more stable plasmas occur in L-mode in the case of higher temperature at the edge and periphery. Global stability analysis performed for the H-mode phase indicates that a lower shear at large radii would help stability and confinement.

Reasonably, the related phenomenology would link together parameters of the plasma edge (recycling and

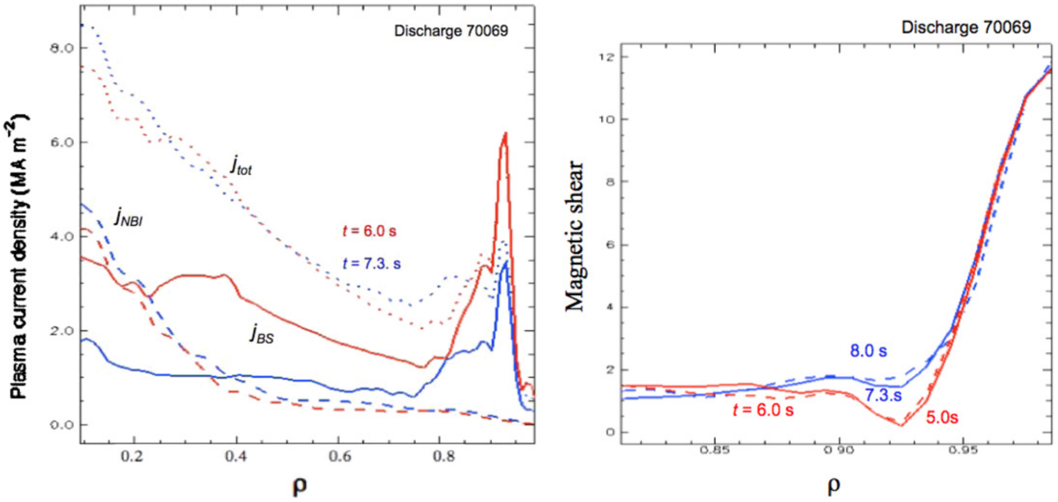

Figure 10. (*a*) Modelling of the plasma current density profile evolution, for discharge 70069 of figure 3. The contributions of NB and bootstrap current density are revealed. Two time points are considered, as representative of the phases of high β_N (at $t = 6.0$ s) and after TB collapse ($t = 7.3$ s). (*b*) Evolution of the magnetic shear radial profile of discharge 70069. The two different time points are representative of the main heating phase in the presence of TB ($t = 5.0$–6.0 s) and after its collapse ($t = 7.3$–8.0 s). The available data averaged over ± 0.5 s at around the nominal time point are considered.

temperature) and periphery (temperature, bootstrap current density, shear) in L-mode that, in turn, are connected to H-mode confinement performance in the core. This interaction suggests that a sort of *virtuous* loop, involving parameters of the edge and periphery, would act and tend to sustain the high-β_N phase. The hypothesized feedback mechanism is favoured by initial conditions of low recycling, high temperature of the edge and periphery and low magnetic shear at large radii, as described hereafter.

High temperature at the edge favours the occurrence of higher $T_{e-\text{periphery}}$ that, in turn, promotes the occurrence of high $j_{BS-\text{periphery}}$ (by the term in expression (4)) and low $s_{\text{periphery}} \approx 0$ in building H-mode profiles consistent with current drive data of figure 10. The relatively high $T_{e-\text{periphery}}$ observed in these regimes should be the consequence of microinstability stabilization that improves confinement via low local shear, resulting in a more stable initial condition of plasma in L mode, as supported by the GENE code results.

The occurrence of some shear increase, detrimental for confinement, could be compensated by a proper self-adjustment of the pressure profile steepness, producing a higher $j_{BS-\text{periphery}}$ sufficient for maintaining the shear low and keeping the system close to the limit of neoclassical transport [33]. In this sense, higher $T_{e-\text{periphery}}$, promoted by low recycling conditions at the beginning of the main heating phase, would help activate the feedback effect. This might explain the link between conditions near the end of the L-mode phase and during the H-mode phase. Since the condition $s_{\text{periphery}} \approx 0$ favours the occurrence of high $T_{e-\text{periphery}}$, once reached, it could, in principle, be self-sustained in SS. Unfortunately, such a *control* mechanism would work in the framework of two opposite effects of high $j_{BS-\text{periphery}}$: one favourable, via stabilizing ballooning modes due to low local shear, the other, detrimental, as it helps in destabilizing low-n MHD modes in the high-β_N plasma [34]. Since the non-inductive current occurring in the experiment is insufficient to fully freeze the current relaxation, the magnetic shear naturally tends to increase at the plasma periphery: consequently, the plasma tends to lose the ballooning stability condition ($s \approx 0$). When this phase of current diffusion is reached, the feedback would produce steeper pressure gradients that are useful for restoring the low shear condition; but, when a certain threshold in steepness is exceeded, the onset of low-n MHD modes occurs, leading to the TB collapse and termination of the high-β_N phase. This picture is consistent with the phenomenology of the high-β_N experiments shown in figures 3 and 4.

With nominal gas fuelling in the prelude, the LHCD effect destroys a suitable condition of low shear at large radii (figure 8(*c*)) that has been provided, instead, by the purely ohmic prelude. The less gas fuelling in prelude restores the useful initial condition via higher temperature of the edge and periphery, which are favoured by lower recycling and promote a higher bootstrap current density at large radii.

Incidentally, the hypothesized feedback mechanism has some analogy with an explanation of the ELM activity via j_{BS}, which produces opposite conditions at the edge for the occurrence of the peeling and ballooning modes [35]. However, in the present context, as found by the transport analysis, the TB penetrates radially deeper in the plasma periphery than in a simple H-mode.

Therefore, we interpret the results linking conditions occurring in the prelude to confinement performance in H-mode as determined by the $q-$and shear profile evolution, since this produces conditions at large radii favourable for stability and confinement.

7. Comments and conclusions

The effect of initial lower recycling on the occurrence of the enhanced β_N period is evidenced by experiments performed with the same operating parameters, in which different initial Dα levels were produced, shot by shot, by means of different gas fuelling waveforms, which however guaranteed the production of the same density in the plasmas prepared for coupling the main heating power. Changes occurring randomly during the experimental session were also monitored. Statistics produced by selecting discharges with only differences in the recycling level at the end of the prelude show that the initial recycling is linked to the maximum β_N value occurring in the H-mode phase.

Modelling in the L-mode phase shows that weaker microinstabilities occur in discharges performed with less gas, lower density and recycling, and higher temperature at the periphery. Available modelling data show that the high-β_N phase is accompanied by high j_{BS} especially at the periphery $\rho \sim 0.9$, which locally produces low magnetic shear. The confinement is significantly improved within a large plasma volume ($\rho 0.8$).

Stability analysis of discharges with a high-β_N phase shows that the confinement performance occurs consistently with a bigger margin in stability due to minimum shear near the plasma edge, in contrast to the worse macroscopic stability case that does not exhibit a significant confinement improvement.

In order to interpret the phenomenology that links initial parameters of the edge and confinement performance, a feedback mechanism has been hypothesized that involves, via the term of relation (4), initial conditions of T_{edge}, $T_{periphery}$, $j_{BS\_periphery}$, $s_{periphery}$ and confinement of the plasma column in H-mode. Following this interpretation, we can conclude that an insufficient current drive would prevent the desired occurrence of a sustained high-β_N phase. In fact, in the considered experiments, the onset of strong MHD event is due to the plasma current that continues to diffuse, despite the relatively high bootstrap current that occurs during the high-β_N phase. On the other hand, it is believable that a further increase in the bootstrap current, e.g. by utilizing a higher main heating power, would produce pressure gradients too steep that are incompatible with the stability of detrimental low-*n* MHD modes. Therefore, the related results of JET indicate that different and more flexible methods for current drive are necessary for the progress of activities foreseen for ITER, aimed at producing regimes of stable plasmas with large volume.

Unfortunately, the LHCD effect was not successfully produced in the experiments considered in this paper, as the configuration of plasma at high triangularity produced high plasma densities even at the edge, and this prevented the penetration of the coupled radio frequency power to the core [12]. However, these profiles represent an important prerequisite for approaching ITER-relevant SS operations and can be used to test the new method for enabling LHCD at reactor-grade high plasma density proved by experiments on FTU (Frascati Tokamak Upgrade) [13]. This method, based on previous theoretical prediction [28, 29], requires a higher temperature at the edge and periphery that can also be obtained by means of low recycling techniques [13]. In fact, a marked change in recycling and temperature at the edge and periphery of an L-mode plasma has already been done in FTU with several methods, including operations with proper gas fuelling waveforms, and producing plasmas with a larger clearance from the walls, thus reducing the plasma–wall interaction with consequent enhancement of the temperature at the edge and periphery. Therefore, the related results represent a baseline for solving the important problem of the lack of penetration of the coupled LH power in the ITER-relevant plasmas of JET with high triangularity.

In summary, operations producing low recycling are useful for enabling the LH current drive effect at reactor graded high plasma density, as well as for promoting regimes with improved confinement in large plasma volumes. Once the parasitic effects preventing the deposition of the coupled LH power at the edge (by the method in [13]) are removed, the LH current drive could efficiently support the bootstrap fraction, thus favouring the sustainment of the high-β_N phase. Next experiments, including those on JET with ITER-like wall should take into account the new method for enabling the LH current drive at high plasma densities.

We have individuated here the more specific aspect of low recycling *as the initial condition (in L-mode) useful for improving performance in H-mode.* Considering that the idea of connecting the recycling to confinement was more recently considered on JET [36], further tests on this issue would be carried out in the next experiments, in particular, in those aimed at developing the hybrid scenario in ITER-like wall [17]. In this regard, the link of initial condition of recycling and confinement performance, found in recent experiments, agrees with statistics produced by data of previous campaigns in carbon wall. Therefore, this behaviour would apply not only to a specific condition of experiment, but it would have a more general validity and could help one to identify a possible new regime of improved confinement in ITER-like wall.

Acknowledgment/Disclaimer

This work was supported by EURATOM and carried out within the framework of the European Fusion Development Agreement. The views and opinions expressed herein do not necessarily reflect those of the European Commission

References

[1] Freidberg J 2007 *Plasma Physics and Fusion Energy* (Cambridge: Cambridge University Press)
[2] Garcia J and Giruzzi G 2012 Conditions for the sustainment of high-beta stationary scenarios in tokamaks *Plasma Phys. Control. Fusion* **54** 015009
[3] Garcia J *et al* 2008 Critical threshold behavior for steady-state internal transport barriers in burning plasmas *Phys. Rev. Lett.* **100** 255004
[4] Garcia J and Giruzzi G 2010 Critical behavior of magnetically confined plasma regimes *Phys. Rev. Lett.* **104** 205003
[5] Fisch N J 1987 Theory of current drive in plasmas *Rev. Mod. Phys.* **59** 175–234
[6] Mailloux J *et al* 2002 *Phys. Plasmas* **9** 2156
[7] Crisanti F *et al* 2002 *Phys. Rev. Lett.* **88** 145004
[8] Castaldo C *et al* 2002 *Phys. Plasmas* **9** 3205
[9] Rimini F G *et al* 2005 *Nucl. Fusion* **45** 1481–92
[10] Litaudon X *et al* 2007 *Plasma Phys. Control. Fusion* **49** B529–50

[11] Mailloux J *et al* 2009 *36th EPS Conf. on Plasma Physics (Sofia, Bulgaria, 29 June–3 July 2009)* vol 33E (ECA) P-5.164
[12] Cesario R *et al* 2011 *Plasma Phys. Control. Fusion* **53** 085011
[13] Cesario R *et al* 2010 *Nature Commun.* **15** 55
[14] Cesario R *et al* 2001 *Phys. Plasmas* **11** 4721
[15] Cesario R *et al* 2002 Operation with low recycling & observation of internal transport barriers sustained by lower hybrid current drive in JET *EFDA-JET Internal Report* PR02
[16] Brezinsek S *et al* 2009 *J. Nucl. Mater.* **390–391** 267–73
[17] Hobirk J *et al* 2009 *36th EPS Conf. on Plasma Physics (Sofia, Bulgaria, 2009)* vol 33E (ECA) O5.057
[18] Challis C D *et al* 2002 *Plasma Phys. Control. Fusion* **44** 1031
[19] Post D E and Behrisch R 1986 *Physics of Plasma–Wall Interactions in Controlled Fusion* (*NATO ASI Series* Series B, Physics) (New York: Plenum)
[20] Zagórski R 1996 *J. Tech. Phys.* **37** 7
[21] Igitkhanov Yu L *et al* 1987 *Proc. 14th EPS Conf. on CFPP (Madrid, Spain)* Part II, p 760
[22] Claaßen H A, Gerhauser H and El-Sharif R N1991 *Report of KFA Jülich* JÜ06L-2423
[23] Igitkhanov Yu L*et al* 1985 *Report of IAE Moscow* 4217/8
[24] Cenacchi G and Taroni A 1986 *Proc. 8th Computational Plasma Physics (Eibsee, Germany, 1986)* EPS vol 10D, p 57
[25] Ida K 1998 *Plasma Phys. Control. Fusion* **40** 1492
[26] Kessel C E 1994 *Nucl. Fusion* **34**
[27] Voitsekovich I *et al* 2009 *Nucl. Fusion* **49** 055026
[28] Cesario R *et al* 2004 *Phys. Rev. Lett.* **92** 175002
[29] Cesario R *et al* 2006 *Nucl. Fusion* **46** 462–76
[30] Mikhailovskii *et al* 1997 *Plasma Phys Rep* **23** 844
[31] Huysmans G *et al* 1990 *Proc. CP90 Conf. on Computational Physics* p 371
[32] Jenko F *et al* 1998 *Phys. Rev. Lett.* **80** 4883
[33] Jackson G L *et al* 1991 *Phys. Rev. Lett.* **67** 3098
[34] Greenfield *et al* 1993 *Plasma Phys. Control. Fusion* **35** B263
[35] Saarelma S *et al* 2000 *Plasma Phys. Control. Fusion* **42** A139–45
[36] Joffrin E *et al* 2010 High confinement hybrid scenario in JET and its significance for ITER*IAEA Conf. (Daejeon, Korea, October 2010)* EXC/1-1